

Solution-processed silicon films and transistors

Tatsuya Shimoda^{1*}, Yasuo Matsuki^{2*}, Masahiro Furusawa^{1*}, Takashi Aoki¹, Ichio Yudasaka¹, Hideki Tanaka¹, Haruo Iwasawa², Daohai Wang², Masami Miyasaka¹ & Yasumasa Takeuchi^{2†}

The use of solution processes—as opposed to conventional vacuum processes and vapour-phase deposition—for the fabrication of electronic devices has received considerable attention for a wide range of applications^{1–7}, with a view to reducing processing costs. In particular, the ability to print semiconductor devices using liquid-phase materials could prove essential for some envisaged applications, such as large-area flexible displays. Recent research in this area has largely been focused on organic semiconductors^{8–11}, some of which have mobilities comparable to that of amorphous silicon¹¹ (a-Si); but issues of reliability remain. Solution processing of metal chalcogenide semiconductors to fabricate stable and high-performance transistors has also been reported^{12,13}. This class of materials is being explored as a possible substitute for silicon, given the complex and expensive manufacturing processes required to fabricate devices from the latter. However, if high-quality silicon films could be prepared by a solution process, this situation might change drastically. Here we demonstrate the solution processing of silicon thin-film transistors (TFTs) using a silane-based liquid precursor. Using this precursor, we have prepared polycrystalline silicon (poly-Si) films by both spin-coating and ink-jet printing, from which we fabricate TFTs with mobilities of $108 \text{ cm}^2 \text{ V}^{-1} \text{ s}^{-1}$ and $6.5 \text{ cm}^2 \text{ V}^{-1} \text{ s}^{-1}$, respectively. Although the processing conditions have yet to be optimized, these mobilities are already greater than those that have been achieved in solution-processed organic TFTs, and they exceed those of a-Si TFTs ($\leq 1 \text{ cm}^2 \text{ V}^{-1} \text{ s}^{-1}$).

We have pursued the development of a novel liquid precursor (herein referred to as 'liquid silicon material') that can be used in a liquid process to form a silicon film^{14,15}. Since the films produced from this precursor must be convertible to high purity silicon, potential candidates are limited to carbon- and oxygen-free hydrogenated silicon compounds. Typical hydrogenated silicon compounds are either of the straight-chain ($\text{Si}_n\text{H}_{2n+2}$) or cyclic (Si_nH_{2n}) forms. For $n \geq 3$, these compounds are liquid at room temperature and decompose to form a-Si when heated to 300°C or higher. However, for $n < 10$, boiling points are less than 300°C and such compounds evaporate before thermal decomposition, which makes solution processing difficult. Oligomeric and polymeric hydrogenated polysilanes, $-(\text{SiH}_2)_n-$, have received little attention since first being synthesized by the Kipping method^{16,17}, because of their limited solubility in organic solvents. Nevertheless, hydrogenated polysilanes are potentially ideal liquid silicon materials provided a suitable solvent can be found. Since cyclic silanes are known to undergo ring-opening polymerization^{18,19}, this reaction can be used for the development of liquid silicon materials. We have applied photo-induced ring-opening polymerization to obtain pure hydrogenated polysilanes from purified hydrogenated cyclic silanes. Among the hydrogenated cyclic silanes we chose cyclopentasilane

(CPS), Si_5H_{10} , since it is relatively stable and exhibits a high photoreactivity upon irradiation with ultraviolet (UV) light.

Using the method developed by Hengge *et al.*^{20,21}, CPS monomer (a clear and colourless liquid under ambient conditions) was synthesized. It has a boiling point of 194°C and is soluble in most organic solvents. After purification, the CPS was exposed to 405 nm UV light to induce photo-polymerization. During exposure, the CPS gradually became cloudy and viscous. After sufficient exposure to the UV source, the liquid was transformed into a white solid, presumably made up of a mixture of hydrogenated polysilanes. Although this solid is insoluble in all common organic solvents, it proved to be soluble in the CPS monomer precursor. The hydrogenated polysilane was also found to dissolve in a mixture of CPS and an organic solvent. This solvent mixture plays an important role in controlling the wettability, coating properties, and thickness of the resulting silicon films, all of which are difficult to control when CPS is used alone. In the actual process, UV irradiation is halted before the CPS completely polymerizes such that polysilanes of various molecular weights are dissolved in unreacted CPS. By diluting the solution with an organic solvent and then filtering out those insoluble polysilanes that precipitated as a result of dilution, we obtained the solution that we refer to as liquid silicon material.

The polymerization process of CPS was investigated using gel permeation chromatography (GPC). Figure 1 shows the results of the GPC measurements of the CPS (Fig. 1a) and the UV-irradiated CPS (Fig. 1b). Peaks corresponding to CPS and toluene were observed in both the non-irradiated and irradiated samples. In addition, in Fig. 1b, a broad peak was also observed around $M_w = 2,600$. This peak corresponds to polysilanes of various molecular weights, indicating CPS polymerization. The GPC measurements were also used to control and optimize the molecular weight distribution of the polysilanes which significantly affects the wettability of the precursor solution to a glass substrate.

The next step is to form an a-Si film by heating the spin-coated polysilane film in order to induce thermal decomposition. Three samples were used to study the thermal decomposition of the polysilane, through the use of thermal desorption spectroscopy (TDS; see Methods). The relationship between the preheating condition of polysilane and the amount of relevant gas (H_2 , SiH_2 and SiH_3) desorbed during the post-annealing phase of TDS are shown in Fig. 2. Sample a, prebaked at 300°C for 10 min, reveals an SiH_2 and SiH_3 desorption peak at around 280°C , followed by intensive hydrogen desorption between 300°C and 400°C , indicating that the polysilane is not completely converted to a-Si when baked at 300°C for 10 min. Given the binding energies of Si–Si (224 kJ mol^{-1}) and Si–H (318 kJ mol^{-1})²², the Si–Si bonds in the polysilane break first at a temperature lower than 280°C , followed next by the breaking of the Si–H bonds, where a three-dimensional silicon network starts to form. In sample b, prebaked at 300°C for 2 h,

¹Technology Platform Research Centre, Seiko Epson Corporation, 281 Fujimi, Fujimi-machi, Nagano-ken, 399-0293 Japan. ²Fine Electronic Research Laboratories, JSR Corporation, 100 Kawajiri-cho, Yokkaichi, Mie, 510-8552 Japan. †Present address: International Centre for Material Research, 1-1 Minamiwataridacho, Kawasaki-ku, Kawasaki-city, Kanagawa, 210-0855 Japan.

*These authors contributed equally to this work.

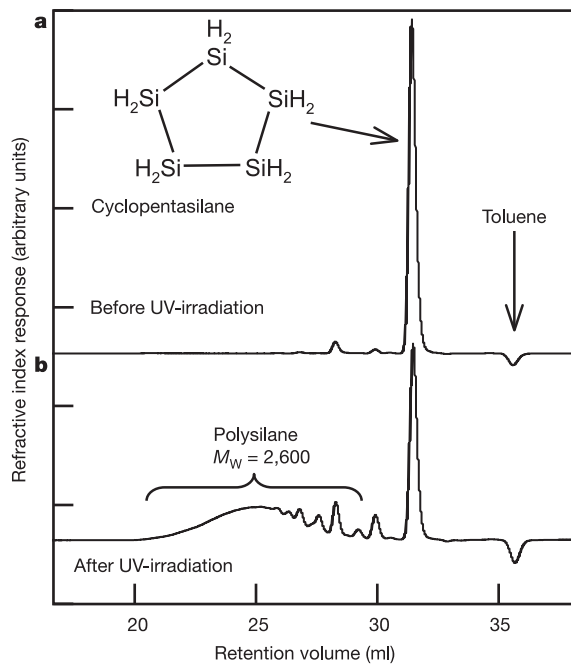


Figure 1 | Gel permeation chromatogram (GPC) of liquid precursor for Si film. **a**, Cyclopentasilane (CPS) and **b**, UV-irradiated CPS, both of which were diluted with toluene (1 vol.%) before GPC measurements. The UV-irradiation conditions were 405 nm, 100 mW cm⁻², and a 10 min irradiation for 1 cm³ of CPS. The broad peak around $M_w = 2,600$ corresponds to polysilanes of various molecular weights as a result of the photo-induced polymerization of CPS.

SiH₂ and SiH₃ desorption is three or four orders of magnitude lower than that of sample a. Sample c released much less desorption gas than samples a and b, since it had almost completely converted to a-Si during preheating at 540 °C for 2 h. Using TDS analysis, we estimate the total amount of hydrogen atoms (the atomic ratio of H/Si) in samples a, b and c, before TDS measurement, to be more than 22%, 3% and 0.3%, respectively. Thus the formation process of a-Si is inferred to be as follows: as the spin-coated polysilane film is heated, volatile components such as toluene and CPS evaporate first. Next, the Si-Si bonds in the polysilane begin to break at a temperature below 280 °C and a fraction of the polysilane is released as SiH₂ and SiH₃. After this, at around 300 °C, the Si-H bonds break, resulting in a three-dimensional a-Si network.

In order to test the electrical properties of the film, we fabricated simplified bottom gate TFTs using the spin-coated a-Si. The maximum mobility of these TFTs was 10⁻³–10⁻⁴ cm² V⁻¹ s⁻¹, which is three or four orders of magnitude smaller than that obtained through conventional plasma enhanced chemical vapour deposition (CVD) techniques. Such poor mobility is attributed to the low concentration of hydrogen atoms that terminate the dangling bonds in the film. Unlike a-Si film formed from conventional CVD, which contains 5–20% hydrogen, the spin-coated a-Si film baked at 540 °C for 2 h contains 0.3% hydrogen and appreciable quantities of dangling bonds that hinder the mobility. In contrast, film that has been spin-coated and baked at a temperature of 300 °C or less contains more than 20% hydrogen and could function somewhat as a semiconductor. However, film processed at such a low temperature might no longer be described as amorphous silicon and is easily oxidized in the air. Some kind of technical solution must be found in order to strike a balance between a lower process temperature and preventing oxidation.

To this end, we have studied the crystallization of the film (before optimization of the low-temperature a-Si process) in order to demonstrate the fundamental potential of this solution processing

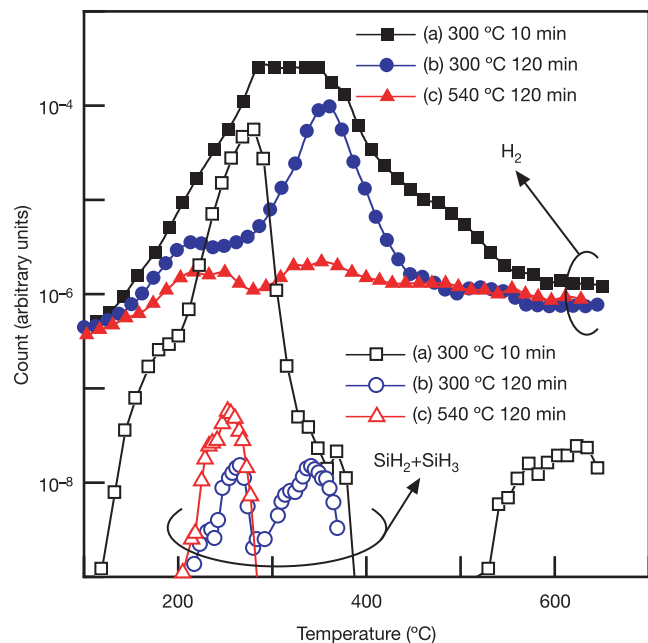


Figure 2 | Thermal desorption spectrum (TDS) of solution-processed a-Si film. Three samples were prepared by the thermal decomposition of polysilane under the following conditions: sample a, 300 °C for 10 min; sample b, 300 °C for 120 min; sample c, 540 °C for 120 min. Desorbed gases from the samples were analysed by mass spectroscopy while the samples were heated in a vacuum.

approach for low-temperature poly-Si (LTPS) TFT applications. In addition, low-hydrogen a-Si films are suitable for excimer laser crystallization, which is the standard crystallization method adopted during the commercial production of LTPS TFTs²³. The a-Si films, formed by coating the liquid silicon material and baking it at 540 °C, were irradiated by a 308 nm XeCl excimer laser at various laser energies. As the laser energy increases, the colour of the films changes from light auburn to light yellow, suggesting a conversion from the amorphous to the polycrystalline phase. The TEM image in Fig. 3 clearly shows the crystalline growth as a result of laser irradiation. Using Raman spectroscopy²⁴, this crystallization process was confirmed to be almost identical to that of a-Si fabricated through conventional CVD. The full-width at half-maximum of the crystalline peak in the Raman spectrum decreases sharply as the laser energy increases, reaching a minimum value of 6.3 cm⁻¹ at around 300 mJ cm⁻²; thereafter the peak slightly broadens, reflecting microcrystallization.

Next, we fabricated TFTs using the coating-formed poly-Si films followed by standard fabrication steps used for conventional LTPS TFTs (see Methods). As shown in Fig. 4a, these TFTs exhibit good electrical characteristics with field-effect mobility (calculated from the transconductance in the saturation region) ranging from 74 to 108 cm² V⁻¹ s⁻¹ in 15 transistors randomly selected among a 4-inch substrate. The transistor of mobility 108 cm² V⁻¹ s⁻¹, whose output characteristics are shown in Fig. 4b, also possesses an on/off ratio of seven digits, 5.0 V in threshold voltage V_{th} and 0.83 V per decade in s -factor (the gate voltage that induces a tenfold increase of drain current in the sub-threshold region).

The mobility was strongly affected not only by the conditions of laser crystallization but also by the amount of oxygen in the silicon film. In the poly-Si film that exhibited a mobility of 108 cm² V⁻¹ s⁻¹ the oxygen concentration was 1,100 p.p.m. Since the CPS and polysilanes are fairly oxygen-sensitive²⁵, several precautions had to be taken during the preparation and treatment of a liquid precursor. The coarsely synthesized CPS was distilled repeatedly to remove impurities including oxides before photo-polymerization.

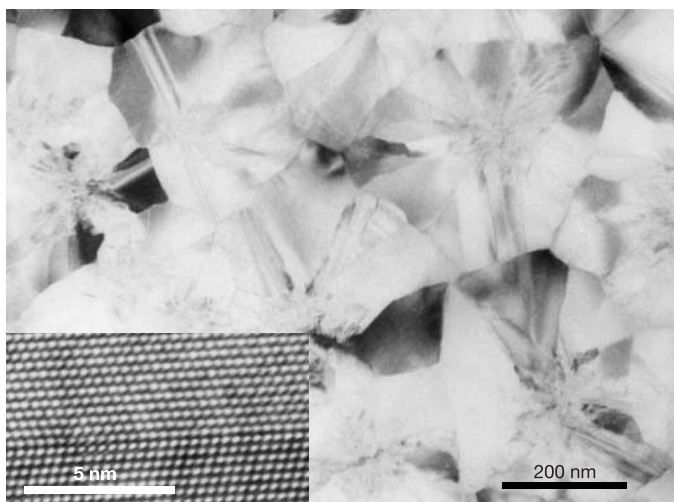


Figure 3 | A TEM image of a solution-processed poly-Si film. The film was formed by spin-coating and baking of the liquid silicon materials followed by laser crystallization. The high-resolution TEM image inserted in the figure clearly highlights the atomic image of the silicon crystal. The micrograph also illustrates that the grain size in the film is about 300 nm, which is comparable to that of conventional CVD-formed poly-Si film.

Furthermore, the organic diluent such as toluene was carefully deoxidized by leaving it in a dry box for several days before use. The oxygen concentration in the box was maintained strictly below 0.5 p.p.m. during all processes from spin-coating to baking. Such precautions enabled control of the oxygen content of the film to less than 2,000 p.p.m. The TFTs resulting from such low-oxygen films exhibited mobility as high as $50\text{--}100\text{ cm}^2\text{ V}^{-1}\text{ s}^{-1}$, while no significant correlations were observed between the oxygen concentration and mobility since manufacturing variations such as the laser condition are the dominant factors. However, a slight failure in controlling the oxygen level in the dry box yielded a silicon film with an oxygen concentration of 8,000 p.p.m. and TFTs with a maximum mobility of $20\text{ cm}^2\text{ V}^{-1}\text{ s}^{-1}$. By intentionally maintaining the oxygen level in the dry box at 10 p.p.m. during all processing, we obtained an insulating a-Si film that contained 7% oxygen.

Finally, we demonstrate the printing applicability of the liquid silicon material by fabricating TFTs using ink-jet formation of poly-Si islands (see Methods). The silicon island can be seen in the SEM image of Fig. 4c as the disk-shaped element with a rough surface. The nature of the external disk-shaped phase with a smooth surface is still unknown, but is presumably the residual remains of the droplet, formed during the drying and shrinking processes, which was once dispersed over the outer disk region. Since the wettability of the liquid silicon material was not sufficiently well understood to enable control of the shrinking behaviour of an ink droplet, the resulting a-Si island became too thick for laser crystallization. A thicker film generally requires a more intense laser for optimal crystallization. The actual laser intensities used for the crystallization of 60 nm spin-coated and 300 nm ink-jet-treated Si film were 345 mJ cm^{-2} and 450 mJ cm^{-2} , respectively. The latter intensity is not optimized but determined roughly from the sample thickness. With such an intense laser source, surface roughness is easily induced, as shown in Fig. 4c.

The ink-jet-printed (or 'ink-jetted') TFT operated with a mobility of $6.5\text{ cm}^2\text{ V}^{-1}\text{ s}^{-1}$ and an on/off ratio of three digits (Fig. 4a). This low mobility is attributed to the poor crystallinity and rough surface, while the large off current, which was confirmed to be the current between source and drain rather than a leak current through the gate insulator, is also attributed to the thick silicon film. Such a thick film contains many dangling bonds and defects near the substrate where crystallization is incomplete. The formation of thin, uniform a-Si film using an ink-jet process would improve the surface morphology

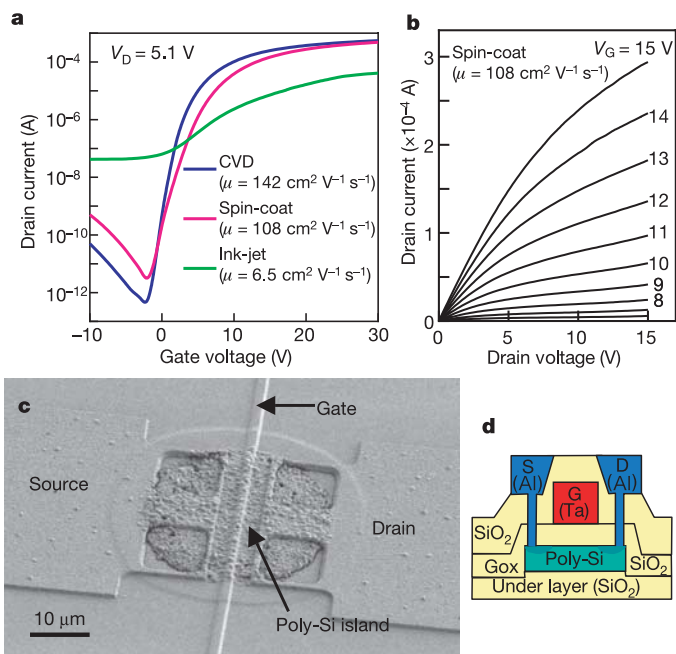


Figure 4 | The structure and characteristics of solution-processed LTPS TFTs. **a**, The transfer characteristics of LTPS TFTs, whose silicon film was formed by CVD (blue), spin-coating (magenta) and ink-jet printing (green), respectively. The drain current of the ink-jetted TFT is normalized to the same channel width and length as the CVD-formed and spin-coated TFTs, for comparison. **b**, The output characteristics of the TFT using spin-coated silicon film whose transfer properties are shown in **a**. **c**, An SEM image of the TFT made from ink-jetted silicon film, whose transfer characteristics are shown in **a**. **d**, A cross-sectional schematic of a fabricated TFT. Gox, SiO_2 gate insulator.

and electrical properties of the poly-Si films. However, the wettability and behaviour of microdroplets are known to differ significantly from those of macroscopic droplets^{26,27}. A thorough understanding of microdroplets will be needed to realize the ink-jet printing of liquid silicon material for practical applications.

We have demonstrated that high-quality poly-Si film can be formed by spin-coating or ink-jetting liquid silicon material. The mobility of the spin-coated TFT, $108\text{ cm}^2\text{ V}^{-1}\text{ s}^{-1}$, is definitely that of an LTPS TFT and cannot be obtained with a-Si TFTs. Though currently inferior to that of conventional spin-coated LTPS TFTs, the performance of our ink-jetted TFT will probably improve with further advances in both the materials and processes employed. The ultimate goal of this research is to fabricate high-performance silicon TFTs by means of an all-liquid process, whereby all layers are directly patterned with liquid materials. To this end, we are currently working to develop liquid materials for films other than channel silicon, such as dielectric layers, doped silicon for source and drain regions, and metallic films for electrodes. The ink-jet process for these materials is also being studied. Such efforts are expected to establish a novel, low-energy, low-cost and high-throughput process for the fabrication of high-performance TFTs.

METHODS

Preparation and analysis of a-Si film. A 30 vol.% toluene solution of UV-irradiated CPS was spin-coated onto a quartz substrate to yield an approximately 100-nm-thick a-Si film after heat treatment. Heat treatment conditions (achieved using a hot plate) for samples a, b and c were $300\text{ }^\circ\text{C}$ for 10 min, $300\text{ }^\circ\text{C}$ for 120 min and $540\text{ }^\circ\text{C}$ for 120 min, respectively. All experiments were carried out in a nitrogen-filled dry box with a residual oxygen concentration of less than 0.5 p.p.m., and the oxygen level was monitored using a galvanic fuel cell sensor. Raman scattering spectra of these samples were recorded in order to confirm the a-Si nature of the films at the typical a-Si peak of around 480 cm^{-1} . Impurity concentrations in the films were investigated using secondary ion mass

spectroscopy. The results confirmed that the film was composed almost entirely of silicon, with only a few trace impurities. Alkali and alkali-earth metal impurities, which negatively affect TFT characteristics, were present at a level of less than 1 p.p.m. The carbon content in the resulting film was surprisingly low—only 200 p.p.m.—considering that an organic solvent was used as the starting material. By strictly controlling the oxygen content in the dry box to less than 0.5 p.p.m., we were able to limit the oxygen content of the film to less than 2,000 p.p.m. Thermal desorption spectroscopy (TDS) was used to investigate the process by which polysilane is converted to a-Si. In TDS, a sample is heated in a vacuum and the gases that are desorbed from the sample are analysed using mass spectroscopy.

Fabrication of TFTs by spin-coating. The n-channel TFTs, whose structure is schematically illustrated in Fig. 4d, were fabricated as follows. First, an SiO₂ underlayer was formed by plasma CVD on a quartz substrate. After cleaning the substrate surface by 172 nm UV-irradiation at 10 mW cm⁻² for 10 min, the liquid silicon material—12 vol.% toluene solution of UV-irradiated CPS—was spin-coated at 2,000 r.p.m. in a nitrogen-filled dry box. The spin-coated substrate was immediately placed on a hot plate heated to 200 °C and the temperature was raised to 400 °C within 10 min. After maintaining a temperature of 400 °C for 30 min, it was further increased to 540 °C over another 10 min period and held for 2 h to form a 50-nm-thick a-Si film. Next, the amorphous film was converted to a polycrystalline one by irradiating it with 308 nm wavelength excimer laser light at 345 mJ cm⁻². After the poly-Si had been etched to create islands, a 120-nm-thick SiO₂ gate insulator (Gox in Fig. 4d) was formed by plasma CVD, followed by tantalum sputtering and etching to form gate electrodes. The source and drain regions were formed by the self-aligned ion implantation of phosphorous ions using the gate electrodes as a mask. Finally, we made the TFTs accessible for measurement by forming an interlayer insulator, opening contact holes in the insulator to reveal the source and drain regions, and then sputtering aluminium to form electrodes. The channel width and length of the TFTs were both 10 μm. The coating-formed silicon film did not present any notable problems or difficulties during the above fabrication steps, as the silicon film was of semiconductor-grade purity and the film processing conditions—etching rate, laser conditions and so on—were nearly the same as those used for CVD-produced silicon film. For comparison, conventional TFTs were fabricated by the same process except that the silicon film was formed by CVD.

Fabrication of TFTs by ink-jet printing. TFTs with the same structure as above were formed using ink-jet printing instead of photolithography to form the channel silicon island. A 10 vol.% toluene solution of UV-irradiated CPS was ink-jet printed on a glass substrate in a nitrogen-filled dry box. This solution was suitable for ejection from a piezo-driven print head¹⁷. Since its viscosity is almost the same as that of toluene and its stability is such that it can be kept for months in a dark place at room temperature, the ejection of the solution from the print head was stable and reproducible. Three droplets, each of weight 10 ng, were deposited in the location where the channel island was to be formed. The droplets were converted into a poly-Si island of diameter 30–40 μm by baking at 540 °C (using the same steps as for spin-coated film) followed by 308 nm excimer laser crystallization at 450 mJ cm⁻². The island was 300 nm thick at the centre and became thinner towards the periphery of the sample. After the gate insulator had been formed, the same steps were applied as for the spin-coated TFTs. The channel width and length of the resulting TFTs were 36 μm and 2 μm, respectively.

Received 20 September 2005; accepted 23 January 2006.

1. Shimoda, T. *et al.* Multicolor pixel patterning of light-emitting polymers by ink-jet printing. In *1999 SID International Symposium Digest of Technical Papers* 376–379 (Society for Information Display, San Jose, 1999).
2. Miyashita, S. *et al.* Full color displays fabricated by ink-jet printing. In *Proc. 21st International Display Research Conference in Conjunction with 8th International Display Workshop (Asia Display / IDW '01)* 1399–1402 (2001).
3. Peumans, P., Uchida, S. & Forrest, S. R. Efficient bulk heterojunction photovoltaic cells using small-molecular-weight organic thin films. *Nature* **425**, 158–162 (2003).

4. Okamura, S., Takeuchi, R. & Shiozaki, T. Fabrication of ferroelectric Pb(Zr,Ti)₃ thin films with various Zr/Ti ratios by ink-jet printing. *Jpn. J. Appl. Phys.* **41**, 6714–6717 (2002).
5. Tahar, R. B. H., Ban, T., Ohya, Y. & Takahashi, Y. Optical, structural, and electrical properties of indium oxide thin films prepared by the sol-gel method. *J. Appl. Phys.* **82**, 865–870 (1997).
6. Yudasaka, I., Tanaka, H., Miyasaka, M., Inoue, S. & Shimoda, T. Poly-Si thin-film transistors using polysilazane-based spin-on glass for all dielectric layers. In *2004 SID International Symposium Digest of Technical Papers* 964–967 (Society for Information Display, San Jose, 2004).
7. Furusawa, M. *et al.* Inkjet-printed bus and address electrodes for plasma display. In *2002 SID International Symposium Digest of Technical Papers* 753–755 (Society for Information Display, San Jose, 2002).
8. Sirringhaus, H. *et al.* High-resolution inkjet printing of all-polymer transistor circuits. *Science* **290**, 2123–2126 (2000).
9. Kawase, T., Sirringhaus, H., Friend, R. H. & Shimoda, T. All-polymer thin film transistors fabricated by high-resolution inkjet printing. In *2000 International Electron Device Meeting (IEDM) Tech. Digest* 623–626 (2000).
10. Gelinck, G. H. *et al.* Flexible active-matrix displays and shift registers based on solution-processed organic transistors. *Nature Mater.* **3**, 106–110 (2004).
11. Afzali, A., Dimitrakopoulos, C. D. & Breen, T. L. High-performance, solution-processed organic thin film transistors from a novel pentacene precursor. *J. Am. Chem. Soc.* **124**, 8812–8813 (2002).
12. Ridley, B. A., Nivi, B. & Jacobson, J. M. All-inorganic field effect transistors fabricated by printing. *Science* **286**, 746–749 (1999).
13. Mitzi, D. B., Kosbar, L. L., Murray, C. E., Copel, M. & Afzali, A. High-mobility ultrathin semiconducting films prepared by spin coating. *Nature* **428**, 299–303 (2004).
14. Aoki, T. *et al.* Method of manufacturing device, device, and electronic apparatus. US Patent Application 0029364 (2004).
15. Shimoda, T. *et al.* Method for forming silicon film. US Patent 6541354 (2003).
16. Kipping, F. S. Organic derivatives of silicon. Complex silicohydrocarbons [SiPh₂]_n. *J. Chem. Soc.* **125**, 2291–2297 (1924).
17. John, P., Oder, I. M. & Wood, J. The electrical conductivity of polysilane, (SiH₂)_x. *J. Chem. Soc. Chem. Commun.* 1496–1497 (1983).
18. Suzuki, M., Kotani, J., Gyobu, S., Kaneko, T. & Saegusa, T. Synthesis of sequence-ordered polysilane by anionic ring-opening polymerization of phenylnonamethylcyclopentasilane. *Macromolecules* **27**, 2360–2363 (1994).
19. Cypryk, M., Gupta, Y. & Matyjaszewski, K. Anionic ring-opening polymerization of 1,2,3,4-tetramethyl-1,2,3,4-tetraphenylcyclopentasilane. *J. Am. Chem. Soc.* **113**, 1046–1047 (1991).
20. Hengge, E. & Bauer, G. Cyclopentasilan, das erste unsubstituierte cyclische Siliciumhydrid. *Angew. Chem.* **85**, 304–305 (1973).
21. Hengge, E. & Bauer, G. Darstellung und Eigenschaften von Cyclopentasilan. *Monatsh. Chem.* **106**, 503–512 (1975).
22. Raabe, G. & Michl, J. Multiple bonding to silicon. *Chem. Rev.* **85**, 419–509 (1985).
23. Sameshima, T., Usui, S. & Sekiya, M. XeCl excimer laser annealing used in the fabrication of poly-Si TFTs. *IEEE Electron Device Lett.* **7**, 276–278 (1986).
24. Kitahara, K., Yamazaki, R., Kurosawa, T., Nakajima, K. & Moritani, A. Analysis of stress in laser-crystallized polysilicon thin films by Raman scattering spectroscopy. *Jpn. J. Appl. Phys.* **41**, 5055–5059 (2002).
25. Chatgililoglu, C. *et al.* Autoxidation of poly(hydrosilane)s. *Organometallics* **17**, 2169–2176 (1998).
26. Morii, K. *et al.* Characterization of light-emitting polymer devices prepared by ink-jet printing. In *Proc. 10th Int. Workshop on Inorganic and Organic Electroluminescence* 357–360 (2000).
27. Morii, K., Masuda, T., Ishida, M., Hotta, S. & Shimoda, T. The direct patterning of crystalline organic-semiconductor films on a substrate by ink-jet printing. In *Proc. Int. Conference on Synthetic Metals* 126–127 (2004).

Acknowledgements We thank the members of Seiko Epson Corporation's pilot line and ink-jet industrial application project, for fabricating TFTs and ink-jet experiments in this research. This work is partially supported by a grant from the New Energy and Industrial Technology Development Organization (NEDO).

Author Information Reprints and permissions information is available at npg.nature.com/reprintsandpermissions. The authors declare no competing financial interests. Correspondence and requests for materials should be addressed to M.F. (furusawa.masahiro@exc.epson.co.jp).